JOURNAL OF MATERIALS SCIENCE 18 (1983) 2743–2751

Young's modulus of Fe-, Co-, Pd- and Pt-based amorphous wires produced by the in-rotating-water spinning method

A. INOUE*, H. S. CHEN, J. T. KRAUSE, T. MASUMOTO†, M. HAGIWARA‡
Bell Laboratories, Murray Hill, New Jersey 07974, USA

This paper presents the Young's modulus of $Fe_{100-x-y}Si_xB_y$, $Fe_{100-x-y}P_xC_y$, $Co_{100-x-y}Si_xB_y$, $Pd_{77.5}Cu_6Si_{16.5}$, $Pd_{48}Ni_{32}P_{20}$ and $Pt_{60}Ni_{15}P_{25}$ amorphous wires determined from the Young's modulus sound velocity measurement. With increasing metalloid content, the Young's modulus increases from 1.58×10^{11} to 1.87×10^{11} N m^{-2} for Fe–Si–B, from 1.40×10^{11} to 1.52×10^{11} N m^{-2} for Fe–P–C and from 1.73×10^{11} to 1.75×10^{11} N m^{-2} for Co–Si–B systems. The increase in Young's modulus with the amount of metalloid elements is the largest for B, followed by Si, C and then P. The Young's modulus of Fe– and Co–Si–B amorphous wires increases significantly with the replacement of iron or cobalt by IV–VII group transition metals. It was recognized that there existed a strong correlation between Young's modulus (E) and tensile fracture strength (σ_f); the ratio of σ_f to E is approximated to be 0.02 for all the amorphous wires investigated. These results imply that the Young's modulus is dominated mainly by the structural and compositional short-range orderings due to the strong interaction between metal and metalloid atoms which hinders the internal displacements. The existence of a constant ratio for σ_f/E was interpreted to originate from a common mechanism for plastic flow of the amorphous wires. Further, it was noted that the Young's modulus of the Fe- and Co-based amorphous wires with diameters of $\simeq$ 100 to 120 μm was slightly lower than that of the amorphous ribbons with thicknesses of $\simeq$ 20 to 25 μm. This difference was attributed to the difference in structural ordering due to the differences in the solidification processes.

1. Introduction

The Young's modulus, which is one of the important engineering characteristics, reflects strongly the interaction and bonding nature among constituent atoms [1]. Its value can be accurately determined within an error of about ± 0.5% by using an ultrasonic technique [2]. Numerous data on the Young's modulus of amorphous alloys of various alloy compositions and strong correlations between Young's modulus and other properties, such as hardness, tensile strength, glass transition temperature and crystallization temperature have been reported [3]. However, all the previous data of Young's modulus for technically interesting Fe- and Co-based amorphous alloys were obtained only from ribbon samples having thickness less than about 40 μm. Recently Hagiwara and co-workers [4–6] have reported, in the alloy systems of Fe–Si–B, Fe–P–C and Co–Si–B, which are very important as an engineering material, the production of continuous amorphous wires up to 200 μm in diameter with uniform circular cross-section. This success appears to promise the extension of practical uses of the amorphous alloys. Since the

*Permanent address: The Research Institute for Iron, Steel and Other Metals, Tohoku University, Sendai 980, Japan.
†The Research Institute for Iron, Steel and Other Metals, Tohoku University, Sendai 980, Japan.
‡Unitika Research Center, Unitika Ltd., Uji 611, Japan.

0022–2461/83 $03.00 + .12

Young's modulus is very sensitive to the disordered state in the amorphous structure, it is very important to determine the Young's modulus of the amorphous wires having a diameter which is about 2 to 10 times as large as that of amorphous ribbons thickness. In this paper, we present the Young's modulus of $Fe_{100-x-y}Si_xB_y$, $Fe_{100-x-y}P_xC_y$, $Co_{100-x-y}Si_xB_y$, $Pd_{77.5}Cu_6Si_{16.5}$, $Pd_{48}Ni_{32}P_{20}$ and $Pt_{60}Ni_{15}P_{25}$ amorphous wires with diameters of 100 to 120 μm produced by the in-rotating-water spinning method.

2. Experimental procedure

Continuous wires of the $Fe_{100-x-y}Si_xB_y$, $Fe_{100-x-y}P_xC_y$, $Co_{100-x-y}Si_xB_y$, $(Fe-M)_{75}Si_{10}B_{15}$, $(Co-M)_{72.5}Si_{12.5}B_{15}$ (M = IV–VII group transition metals), $Pd_{77.5}Cu_6Si_{16.5}$, $Pd_{48}Ni_{32}P_{20}$ and $Pt_{60}Ni_{15}P_{25}$ alloys, typically 100 to 120 μm in diameter, were synthesized directly from the melt by using an in-rotating-water spinning method [7, 8] and confirmed to be amorphous by conventional X-ray diffraction and optical microscopy. The subscripts refer to the atomic percentages of the constituents. The sound velocity (V_E) was measured at 100 kHz using a pulse-echo technique on amorphous wires about 50 to 100 cm long and Young's modulus (E) was given by $E = \rho V_E^2$, where ρ is the density of the amorphous wire. The measurement was conducted at ambient temperatures. The detailed procedure has been described previously [2]. For ferromagnetic samples, the velocity was measured in a saturating magnetic field parallel to the sample lengths. The sound velocity reached a maximum plateau with an applied field of about 50 Oe. The maximum value was used for the Young's modulus determination. The maximum scatter of the velocity measurement was estimated to be ± 0.5% due to the uncertainties in length measurements.

TABLE I Sound velocity V_E, Young's modulus E, density ρ, tensile fracture strength σ_f, Vickers hardness H_v, tensile fracture strain $\epsilon_f = \sigma_f/E$, yield strain $\epsilon_y \simeq H_v/3E$ and crystallization temperature T_x for Fe–Si–B, Fe–P–C and Co–Si–B amorphous wires. Data of σ_f, H_v and T_x are from [4–6]

Alloy composition (at %)	V_E (km sec^{-1})	E (10^{10} N m^{-2})	ρ (10^3 kg m^{-3})	σ_f (10^8 N m^{-2})	H_v (10^8 N m^{-2})	$\epsilon_f = \sigma_f/E$ (%)	$\epsilon_y = H_v/3E$ (%)	T_x (K)
$Fe_{80}Si_{10}B_{10}$	4.655	15.8	7.27	29.1	81.3	1.8	1.7	750
$Fe_{80}Si_5B_{15}$	4.749	16.5	7.30	33.2	85.3	2.0	1.7	763
$Fe_{77.5}Si_{10}B_{12.5}$	4.773	16.4	7.21	31.0	91.6	1.9	1.9	793
$Fe_{77.5}Si_{7.5}B_{15}$	4.816	16.8	7.23	32.7	88.2	1.9	1.8	789
$Fe_{75}Si_{10}B_{15}$	4.884	17.1	7.16	34.1	101	2.0	2.0	805
$Fe_{75}Si_{15}B_{10}$	4.765	16.1	7.11	31.7	90.2	2.0	1.9	793
$Fe_{75}Si_{12.5}B_{12.5}$	4.822	16.6	7.14	32.0	94.1	1.9	1.9	800
$Fe_{75}Si_{7.5}B_{17.5}$	4.911	17.3	7.17	35.6	94.1	2.1	1.8	798
$Fe_{72.5}Si_{12.5}B_{15}$	4.931	17.2	7.08	33.5	102	1.9	2.0	812
$Fe_{72.5}Si_{10}B_{17.5}$	5.000	17.8	7.10	33.1	102	1.9	1.9	805
$Fe_{70}Si_{10}B_{20}$	5.156	18.7	7.05	39.2	108	2.1	1.9	805
$Fe_{80}P_{12.5}C_{7.5}$	4.410	14.0	7.27	27.3	79.4	2.0	1.9	682
$Fe_{77.5}P_{17.5}C_5$	4.384	14.2	7.16	27.6	77.0	1.9	1.8	694
$Fe_{77.5}P_{15}C_{7.5}$	4.423	14.0	7.20	27.6	76.5	2.0	1.8	690
$Fe_{77.5}P_{12.5}C_{10}$	4.404	14.1	7.25	27.9	79.9	2.0	1.9	692
$Fe_{77.5}P_{10}C_{12.5}$	4.386	14.0	7.30	28.3	79.9	2.0	1.9	694
$Fe_{77.5}P_{7.5}C_{15}$	4.481	14.3	7.34	29.8	80.9	2.1	1.9	693
$Fe_{75}P_{15}C_{10}$	4.470	14.4	7.23	28.2	79.4	2.0	1.8	706
$Fe_{75}P_{12.5}C_{12.5}$	4.429	14.1	7.23	28.3	83.4	2.0	2.0	694
$Fe_{75}P_{10}C_{15}$	4.558	15.2	7.28	29.9	87.8	2.0	1.9	706
$Co_{77.5}Si_{12.5}B_{10}$	4.918	19.0	7.85	35.8	112	1.9	2.0	688
$Co_{77.5}Si_{7.5}B_{15}$	4.771	18.1	7.96	32.7	135	1.8	2.5	686
$Co_{75}Si_{15}B_{10}$	4.731	17.3	7.72	30.3	110	1.8	2.1	766
$Co_{75}Si_{10}B_{15}$	4.714	17.4	7.85	31.8	105	1.8	2.0	774
$Co_{72.5}Si_{12.5}B_{15}$	4.731	17.4	7.74	34.5	111	2.0	2.1	791
$Co_{70}Si_{15}B_{15}$	4.792	17.5	7.60	30.2	115	1.7	2.2	811
$Pd_{77.5}Cu_6Si_{16.5}$	2.918	8.78	10.3	15.6	38.0	1.8	1.4	680
$Pd_{48}Ni_{32}P_{20}$	3.099	9.57	10.07	–	46.0	–	1.6	645
$Pt_{60}Ni_{15}P_{25}$	2.439	9.35	15.71	–	37.5	–	1.3	524

The densities (ρ) were assumed to be the same as the previous values [9–12] of amorphous ribbons which were measured by the liquid displacement technique. Tensile fracture strength (σ_f), hardness (H_v) and crystallization temperature (T_x) of the amorphous wires were taken from [4–6].

3. Results

The sound velocity (V_E) and Young's modulus (E) of the Fe–Si–B, Fe–P–C, Co–Si–B, Pd–Cu–Si, Pd–Ni–P and Pt–Ni–P amorphous wires are listed in Table I, where the data of density (ρ), tensile fracture strength (σ_f), Vickers hardness (H_v), tensile fracture strain ($\epsilon_f = \sigma_f/E$), tensile yield strain ($\epsilon_y \simeq H_v/3E$) and crystallization temperature (T_x) are also shown for comparison. The approximation of $\epsilon_y \simeq H_v/3E$ is based on the fact that amorphous alloys exhibit little work-hardening and thus the tensile flow strength is related by $\sigma_f \simeq 1/3H_v$ [13]. Figs. 1 to 3 show compositional dependencies of the Young's modulus for Fe–Si–B, Fe–P–C and Co–Si–B amorphous wires having diameters of 100 to 120 μm. With increasing metalloid content, the Young's modulus showed an appreciable increase from 1.58×10^{11} to 1.87×10^{11} N m^{-2} for Fe–Si–B system, and from 1.40×10^{11} to 1.52×10^{11} N m^{-2} for Fe–P–C system but was seen to increase only slightly (from 1.73×10^{11} to 1.75×10^{11} N m^{-2}) for the Co–Si–B system. We noted abnormally high modulus values in the Co–Si–B alloys with low metalloid compositions. Considering the fact that the diameters of the low metalloid-containing alloys are almost equal to those [14] of maximum ribbon thicknesses for the formation of an amorphous phase, the abnormally high Young's modulus values appear to be due to the precipitation of small amounts of cystalline phases even though no precipitation is detected by conventional X-ray diffraction and optical microscopy. The highest value of Young's modulus in each alloy system decreases in the order of Fe–Si–B > Co–Si–B > Fe–P–C, in agreement with the orders [4–6] of hardness and tensile fracture strength. The highest Young's modulus of Fe–Si–B amorphous wires reaches a value as high as about 1.9×10^{11} N m^{-2} which is comparable to that of pure iron and nickel. Figs. 1 and 2 also show that the influence of the metalloid elements on the increase of Young's modulus for the Fe-based amorphous wires is the largest for boron, followed by silicon, carbon and then phosphorus, indicating that the atomic ordering between iron and boron is much

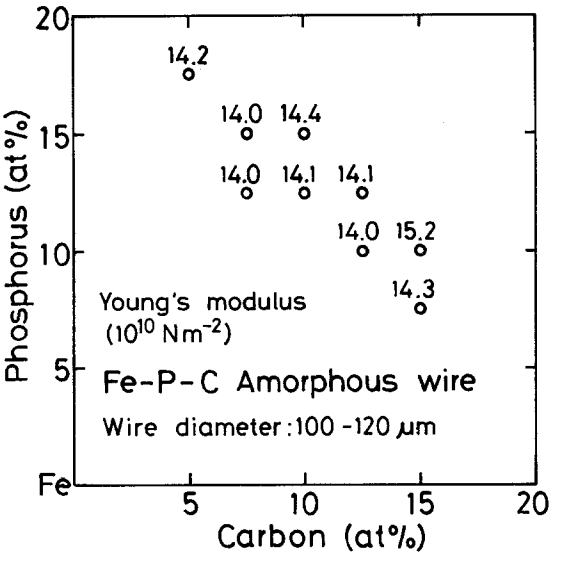

Figure 2 Compositional dependence of the Young's modulus for Fe–P–C amorphous wires.

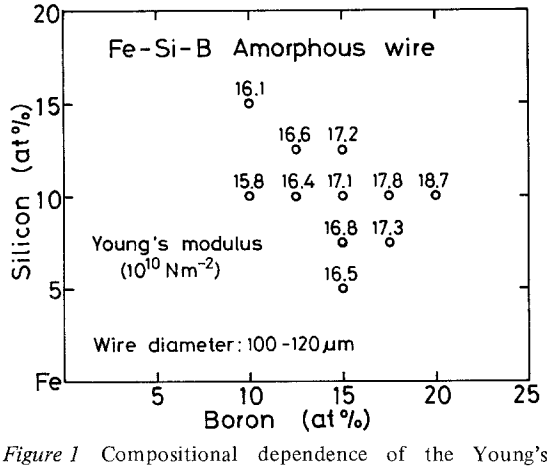

Figure 1 Compositional dependence of the Young's modulus for Fe–Si–B amorphous wires.

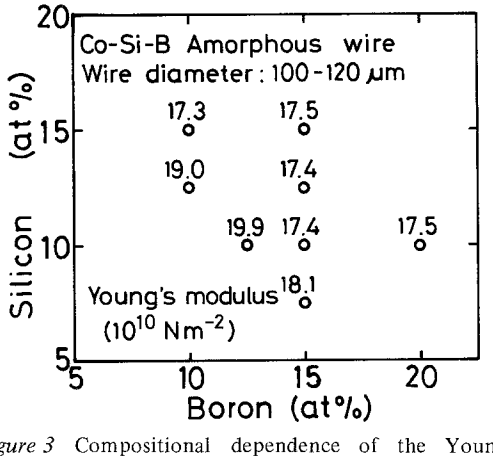

Figure 3 Compositional dependence of the Young's modulus for Co–Si–B amorphous wires.

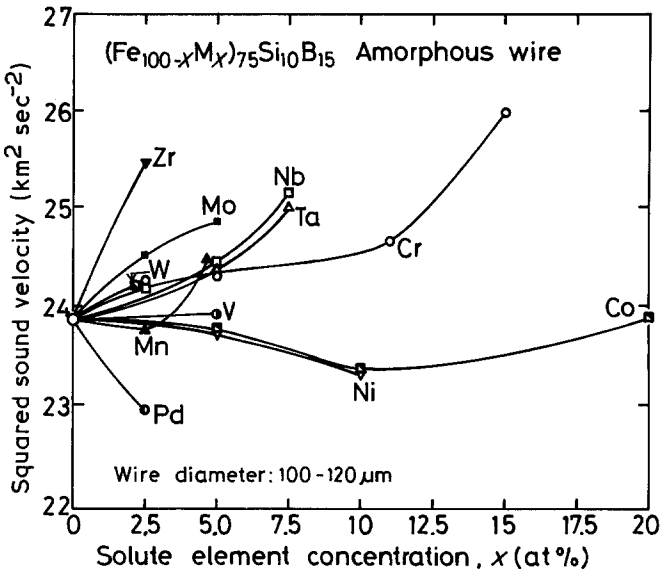

Figure 4 Change in the squared sound velocity for $(Fe_{100-x}M_x)_{75}Si_{10}B_{15}$ amorphous wires with the content of transition metal, M = Zr, V, Nb, Ta, Cr, Mo, W, Mn, Co, Ni or Pd.

stronger than that between iron and other metalloids. This tendency is similar to that of the σ_f and H_v for the amorphous wires [4, 6]. Such an influence of the metalloids on the Young's modulus may be interpreted as follows: the Young's modulus is dominated primarily by the bond stiffnesses which reflect the strength of the chemical interaction between metal and metalloid atoms rather than that between the metal components themselves. However, one may note in Fig. 3 that an increasing boron content shows little effect on the Young's modulus for Co–Si–B wires. This

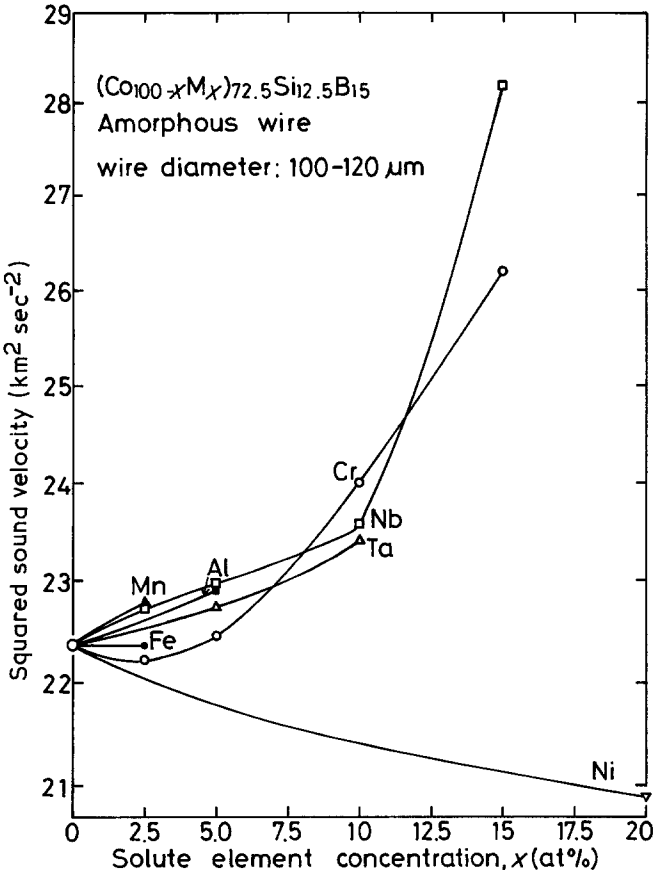

Figure 5 Change in the squared sound velocity for $(Co_{100-x}M_x)_{72.5}Si_{12.5}B_{15}$ amorphous wires with the content of transition metal, M = V, Nb, Ta, Cr, Mo, Mn, Fe or Ni.

behaviour may be attributed to the electronic contribution to the modulus softening compensating the increase in Young's modulus due to atomic ordering [15]. In the Co–B–Si amorphous alloys, electronic configuration of d-shell orbitals alters drastically with boron addition as evidenced by the lowering of magnetic moments and Curie temperatures.

Since there are no density data available, Figs. 4 and 5 show the change in squared sound velocity $V_E^2 = E/\rho$ (in place of E) of $(Fe–M)_{75}Si_{10}B_{15}$ and $(Co–M)_{72.5}Si_{12.5}B_{15}$ amorphous wires with the replacement of iron or cobalt by IV–VIII group transition metals of the periodic table. The compositional dependence is, in many respects, similar for both the alloy series; e.g. (a) the solute elements which raise the sound velocity are located at the left hand side of iron or cobalt in the periodic table, (b) no significant effect is seen in the mixing between iron and cobalt, and (c) the addition of the solute M elements such as nickel and palladium, which are located at the right hand side of iron and cobalt in the periodic table, results in a decrease in the sound velocity. Judging from the fact [16] that the Young's modulus of zirconium, niobium and tantalum elements themselves is lower than that of iron and cobalt metals, it may be concluded that the effect of the metal solute elements on the velocity of the resultant amorphous alloys originates from the strong interaction between the solute metal and the metalloid atoms.

The Young's modulus of the Pd- and Pt-based wires is $8.77 \times 10^{10} N m^{-2}$ for $Pd_{77.5}Cu_6Si_{16.5}$, $9.62 \times 10^{10} N m^{-2}$ for $Pd_{48}Ni_{32}P_{20}$ and $9.35 \times 10^{10} N m^{-2}$ for $Pt_{60}Ni_{15}P_{25}$ and decreases in the order of $Pd_{48}Ni_{32}P_{20} > Pt_{60}Ni_{15}P_{25} > Pd_{77.5}Cu_6Si_{16.5}$. These values are slightly lower than the previously reported values ($10.16 \times 10^{10} N m^{-2}$ for $Pd_{48}Ni_{32}P_{20}$, $9.61 \times 10^{10} N m^{-2}$ for $Pt_{60}Ni_{15}P_{25}$ and $9.29 \times 10^{10} N m^{-2}$ for $Pd_{77.5}Cu_6Si_{16.5}$) [13] for the amorphous alloys with a cylindrical geometry produced by quenching in water the molten alloys contained in a drawn fused-silica capillary. Although the difference in the Young's modulus is rather small, it may be due to the result that the Pd- and Pt-based wires produced by the in-rotating-water spinning method have a more disordered structure, in which the degree of the short-range ordering is lower, owing to the much smaller cross-sectional size and the much higher quenching rate obtained by the present melt spinning apparatus.

4. Discussion

It is expected that the Young's modulus, which reflects the ease of internal displacement, strongly correlates to the tensile fracture strength σ_f and hardness H_v. Based on the data of E, σ_f and H_v for Fe–Si–B, Fe–P–C, Co–Si–B, Pd–Cu–Si, Pd–Ni–P and Pt–Ni–P amorphous wires listed in

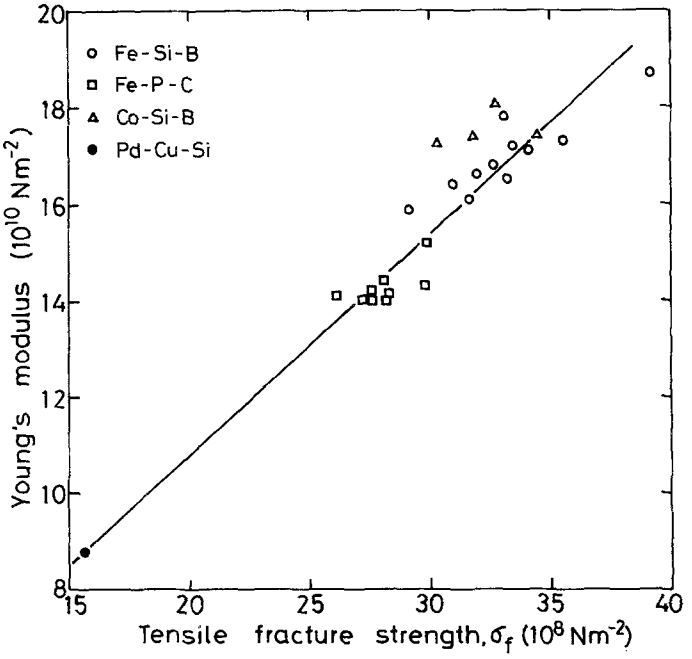

Figure 6 The correlation between Young's modulus and tensile fracture strength (σ_f) for Fe–Si–B, Fe–P–C, Co–Si–B and $Pd_{77.5}Cu_6Si_{16.5}$ amorphous wires. Data of σ_f are from [4–6, 8].

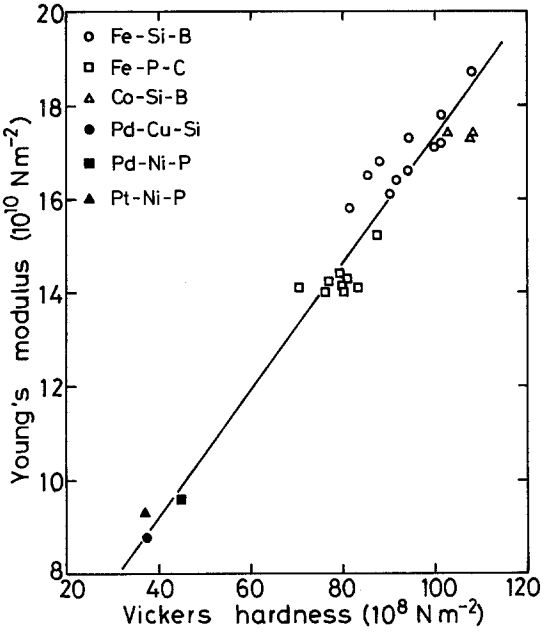

Figure 7 The correlation between Young's modulus and Vickers hardness (H_v) for Fe–Si–B, Fe–P–C, Co–Si–B, $Pd_{77.5}Cu_6Si_{16.5}$, $Pd_{48}Ni_{32}P_{20}$ and $Pt_{60}Ni_{15}P_{25}$ amorphous wires. Data of H_v are from [4–6, 8, 16].

Table I, the E values are plotted as a function of σ_f and H_v in Figs. 6 and 7. The data points are located in a scatter band following a roughly linear relationship even though the slope is such that the relationship does not extrapolate to the origin. This tendency is consistent with that of the amorphous ribbon samples in metal–metalloid and metal–metal alloy systems [14, 16–22]. It is noteworthy in Table I and Fig. 6 that the observed ratio of σ_f to E shows an almost constant value of about 0.020 for all amorphous wires investigated, in spite of significant differences in σ_f as well as E. On the other hand, the ratio of $H_v/3$ to E is about 0.020 for the Fe–Si–B, Fe–P–C and Co–Si–B wires, but the values for the Pd- and Pt-based amorphous wires are considerably lower ($\simeq 0.015$), in agreement with the tendency for amorphous ribbon samples [15]. The observed ratio of E to σ_f is nearly equal to 50. This value is much smaller than that (100 to 200) of conventional steels and may be comparable to that (15.5) or iron whiskers [23]. A similar strong correlation between E/ρ and σ_f was obtained for the series of $(Fe–M)_{75}Si_{10}B_{15}$ and $(Co–M)_{72.5}Si_{12.5}B_{15}$ amorphous wires as manifested in Fig. 8. The following two features are derived from this result: (a) increasing σ_f is associated with an increasing stiffness and the mechanism of such changes is the same between E and σ_f, and (b) there is no evident change in the plastic flow mechanism for all of the amorphous alloys. Accordingly, it may be concluded that the variation in E with alloy composition is not due to the difference in flow mechanism but attributed to the change in the short-range ordering.

We examine next the influence of transition metals on the Young's modulus velocity in the series of $(Fe–M)_{75}Si_{10}B_{15}$ and $(Co–M)_{72.5}Si_{12.5}B_{15}$ amorphous wires. Previous studies [24] have pointed out the importance of the average group number (AGN) of metallic atoms in amorphous alloys in an understanding of the effect of transition metals on the σ_f, H_v and T_x. We found, in fact, that the sound velocity was also significantly influenced by the AGN. In Fig. 9, the measured

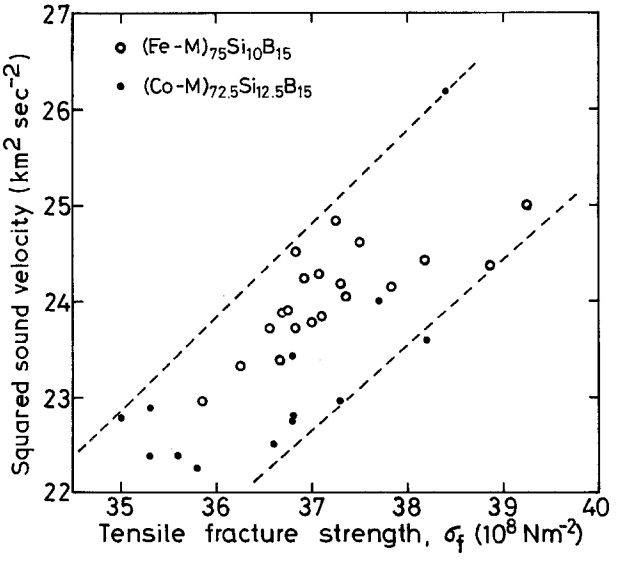

Figure 8 The correlation between squared sound velocity and tensile fracture strength σ_f for $(Fe_{100-x}M_x)_{75}Si_{10}B_{15}$ and $(Co_{100-x}M_x)_{72.5}Si_{12.5}B_{15}$ amorphous wires. Data of σ_f are from [4, 6].

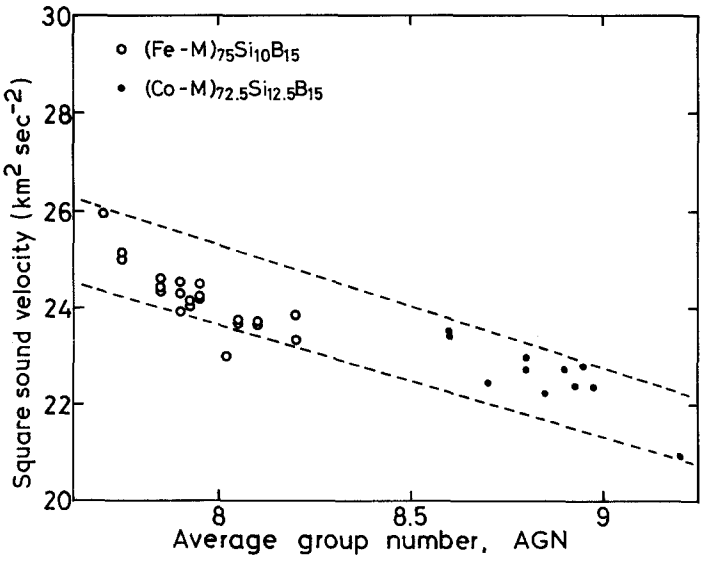

Figure 9 Change in the squared sound velocity of $(Fe_{100-x}M_x)_{75}Si_{10}B_{15}$ and $(Co_{100-x}M_x)_{72.5}Si_{12.5}B_{15}$ amorphous wires with the average group number of metallic atom (AGN), M = Zr, V, Nb, Ta, Cr, Mo, W, Mn, Fe, Co, Ni or Pd.

values of squared sound velocity are plotted against the AGN (average ratio of outer s + d electrons to atoms) of metallic atoms in the amorphous wires. By taking the numbers of the outer electrons to be 4 for zirconium, 5 for vanadium, niobium and tantalum, 6 for chromium, molybdenum and tungsten, 7 for manganese, 8 for iron, 9 for cobalt and 10 for nickel and palladium, respectively, the AGN was given by the weighted means according to the atomic percentage of the transition elements. The strong dependence of the Young's modulus sound velocity on AGN that persists even though there is rather large scatter in the data implies that structural and compositional orderings due to the strong interaction between metal and metalloid atoms play an important role in the large change of Young's modulus of the Fe- and Co-based amorphous wires. The compositional ordering has been considered to arise from the strong interactions among unlike atoms [25] and the strong affinity between unlike atoms is manifested by a large negative heat of mixing as evidenced by the existence of high melting intermetallic compounds and the deep valley of melting temperature around an eutectic composition in the transition metal (M) of silicon and boron alloys.

TABLE II Comparisons of sound velocity V_E and Young's modulus E in the ribbon and wire samples for $Fe_{75}Si_{10}B_{15}$, $Fe_{77.5}P_{12.5}C_{10}$, $Co_{72.5}Si_{12.5}B_{15}$, $Pd_{77.5}Cu_6Si_{16.5}$, $Pd_{48}Ni_{32}P_{20}$ and $Pt_{60}Ni_{15}P_{25}$ amorphous wires

Alloy composition (at %)	Thickness or diameter (μm)	V_E (km sec^{-1})	E (10^{10} N m^{-2})	Ratio of change (%)
$Fe_{75}Si_{10}B_{15}$				
ribbon	$\simeq$ 20	4.967	17.7	−3.4
wire	$\simeq$ 120	4.884	17.1	
$Fe_{77.5}P_{12.5}C_{10}$				
ribbon	$\simeq$ 20	4.423	14.2	−0.7
wire	$\simeq$ 110	4.404	14.1	
$Co_{72.5}Si_{12.5}B_{15}$				
ribbon	$\simeq$ 23	4.762	17.6	−1.1
wire	$\simeq$ 100	4.731	17.4	
$Pd_{77.5}Cu_6Si_{16.5}$				
ribbon	$\simeq$ 25	2.920	8.78	−0.1
wire	$\simeq$ 105	2.918	8.77	
$Pd_{48}Ni_{32}P_{20}$				
ribbon	$\simeq$ 15	3.083	9.57	+0.5
wire	$\simeq$ 115	3.092	9.62	
$Pt_{60}Ni_{15}P_{25}$				
ribbon	$\simeq$ 20	2.439	9.35	0
wire	$\simeq$ 115	2.439	9.35	

Lastly, we investigated the difference of Young's modulus between the ribbon samples having thicknesses of 15 to 25 μm and the wire samples having diameters of 100 to 120 μm. The Young's modulus and the sound velocity in the ribbon and wire forms for $Fe_{75}Si_{10}B_{15}$, $Fe_{77.5}P_{12.5}C_{10}$, $Co_{72.5}Si_{12.5}B_{15}$, $Pd_{77.5}Cu_6Si_{16.5}$, $Pd_{48}Ni_{32}P_{20}$ and $Pt_{60}Ni_{15}P_{25}$ alloys are listed in Table II, where the data of ribbon thicknesses and wire diameters are also shown for comparison. Considering the result that the maximum uncertainty of the sound velocity is about $\pm 0.5\%$, it is concluded that the Young's modulus of the ribbon and wire samples is, within experimental uncertainty, the same amoung $Pd_{77.5}Cu_6Si_{16.5}$, $Pd_{48}Ni_{32}P_{20}$ and $Pt_{60}Ni_{15}P_{25}$ alloys. It is rather striking that the Young's modulus of $Fe_{75}Si_{10}B_{15}$, $Fe_{77.5}P_{12.5}C_{10}$ and $Co_{72.5}Si_{12.5}B_{15}$ alloys is larger by 3.4, 0.7 and 1.1%, respectively, for the ribbon samples than for the wire samples, since it has been generally recognized that the Young's modulus increases by structural relaxation on annealing at temperatures well lower than T_x [26] and with increasing ribbon sample thickness [27] or wire diameter [27]. That is, it may be said that the larger the degree of the structural disorder the smaller is the Young's modulus. Accordingly, it may be said that the wire samples ($\geqslant 100\,\mu$m diameter) of $Fe_{75}Si_{10}B_{15}$, $Fe_{77.5}P_{12.5}C_{10}$ and $Co_{72.5}Si_{12.5}B_{15}$ alloys have a more disordered structure compared with the ribbon samples ($\leqslant 25\,\mu$m thickness).

It has been reported that the maximum ribbon thickness for the formation of an amorphous phase by the conventional single roller quenching technique is usually less than about 40 μm [28], whereas the maximum wire diameter for the formation of an amorphous phase by the in-rotating-water spinning method is about 270 μm for $Fe_{75}Si_{10}B_{15}$ [4], about 230 μm for $Fe_{77.5}P_{12.5}C_{10}$ [5] and about 140 μm for $Co_{72.5}Si_{12.5}B_{15}$ alloys [6]. Therefore, it appears that the wire samples exhibited Young's moduli lower than those of the ribbon samples due to the much larger amorphous-forming capacity for the in-rotating-water spinning method. The larger capacity is considered to originate from the inherent differences in the solidification process of the ejected melt as well as in the manner of cooling after solidification: that is, in the case of the single roller quenching method, the solidification of the melt is achieved only through contact with the roller [29] with contacting time and length for Fe–Si–B alloys as short as about 0.01 sec and 100 mm, respectively [30]. The solidified ribbon detaches itself from the roller at or above the glass transition and is air-cooled to room temperature. On the other hand, in the in-rotating-water spinning method, the rapidly circulating water cools the melt continuously over the entire outside surface of the wire [7, 8, 31]. The slight differences in the Young's moduli observed between the wire and ribbon samples of the Pd- and Pt-based alloys is probably a result of lower glass temperatures and thus less structural relaxation during cooling after solidification as compared with the Fe- and Co-based alloys.

5. Summary and conclusions

The Young's modulus of $Fe_{100-x-y}Si_xB_y$, $Fe_{100-x-y}P_xC_y$, $Co_{100-x-y}Si_xB_y$, $Pd_{77.5}Cu_6Si_{16.5}$, $Pd_{48}Ni_{32}P_{20}$ and $Pt_{60}Ni_{15}P_{25}$ amorphous wires produced by the in-rotating-water spinning method was determined by measuring the sound velocity of the wire with the pulse-echo technique. The Young's modulus increases from 1.58×10^{11} to $1.87 \times 10^{11}\,N\,m^{-2}$ for Fe–Si–B, from 1.40×10^{11} to $1.52 \times 10^{11}\,N\,m^{-2}$ for Fe–P–C and from 1.73×10^{11} to $1.75 \times 10^{11}\,N\,m^{-2}$ for Co–Si–B with increasing metalloid content. The influence of metalloid elements on the increase in the Young's modulus of the Fe-based alloys was much larger for boron as compared with the other metalloids.

The Young's molulus of Fe–Si–B and Co–Si–B amorphous wires increased significantly with the replacement of iron or cobalt by transition metals having an averaged group number less than 8. From the compositional dependencies of the Young's modulus, it was concluded that the short-range ordering due to the strong chemical bonding nature between metal and metalloid atoms influences significantly the Young's modulus. The Young's modulus of the Pd- and Pt-based amorphous wires ranges from 8.8×10^{10} to $9.6 \times 10^{10}\,N\,m^{-2}$, being much lower than those of the Fe- and Co-based wires. There exists a strong correlation between the Young's modulus and the tensile fracture strength for all the amorphous wires and the ratio of σ_f/E shows a constant value ($\simeq 0.02$) in spite of large differences in E and σ_f. It was interpreted that the strong correlation originates from a common mechanism for plastic flow among all the amorphous wires.

It was found that there is no difference in Young's modulus between the amorphous wires

and ribbons for the Pd- and Pt-based alloys, whereas the E values of Fe–Si–B, Fe–P–C and Co–Si–B alloys are slightly lower for the wire samples having diameters of 100 to 120 μm than for the ribbon samples having thicknesses of 20 to 25 μm. This finding is rather striking and was interpreted as a result of structural ordering due to the significant difference in the solidification processes of the melt, particularly the cooling process after solidification of the wire and ribbon samples.

Acknowledgements

The authors would like to thank Mr H. Tomioka of Unitika Ltd for producing some amorphous wires.

References

1. W. KÖSTER and H. FRÄNZ, *Met. Rev.* **6** (1961) 1.
2. J. T. KRAUSE and H. S. CHEN, Proceedings of 2nd International Conference on Rapidly Quenched Metals, Cambridge, November 1975, edited by N. J. Grant and B. C. Giessen (MIT Press, Cambridge, Mass. 1976) p. 425.
3. H. S. CHEN, *Rep. Prog. Phys.* **43** (1980) 353.
4. M. HAGIWARA, A. INOUE and T. MASUMOTO, *Met. Trans.* **13A** (1982) 373.
5. A. INOUE, M. HAGIWARA and T. MASUMOTO, *J. Mater. Sci.* **17** (1982) 580.
6. M. HAGIWARA, A. INOUE and T. MASUMOTO, *Mater. Sci. Eng.* **54** (1982) 197.
7. I. OHNAKA, T. FUKUSAKO and T. DAIDO, *J. Jpn. Inst. Met.* **45** (1981) 751.
8. T. MASUMOTO, I. OHNAKA, A. INOUE and M. HAGIWARA, *Scripta Metall.* **15** (1981) 293.
9. K. SHIRAKAWA, Y. WASEDA and T. MASUMOTO, *Sci. Rep. Res. Inst. Tohoku Univ.* **29A** (1981) 229.
10. K. ASO, M. HAYAKAWA, K. HOTAI, S. UEDAIRA, Y. OCHIAI and Y. MAKINO, Proceedings of the 4th International Conference on Rapidly Quenched Metals, Sendai, August 1981, edited by T. Masumoto and K. Suzuki (The Japan Institute of Metals, Sendai 1982) p. 379.
11. H. S. CHEN, unpublished research (1978).
12. K. SHIRAKAWA, private communication (1982).
13. H. S. CHEN, J. T. KRAUSE and E. COLEMAN, *J. Non-Cryst. Solids* **78** (1975) 157.
14. M. HAGIWARA, A. INOUE and T. MASUMOTO, *Sci. Rep. Res. Inst. Tohoku Univ.* **29A** (1981) 351.
15. H. S. CHEN, *J. Appl. Phys.* **49** (1978) 462.
16. "Metals Databook", edited by The Japan Institute of Metals, Maruzen, Tokyo (1974) p. 35.
17. L. A. DAVIS, *Scripta Metall.* **9** (1975) 431.
18. H. S. CHEN, *Mater. Sci. Eng.* **26** (1976) 79.
19. L. A. DAVIS, C. P. CHOU, L. E. TANNER and R. RAY, *Scripta Metall.* **10** (1976) 937.
20. T. MASUMOTO, *Sci. Rep. Res. Inst. Tohoku Univ.* **26A** (1977) 246.
21. S. H. WHANG, D. E. POLK and B. C. GIESSEN, Proceedings of the 4th International Conference on Rapidly Quenched Metals, Sendai, August 1981, edited by T. Masumoto and K. Suzuki (The Japan Institute of Metals, Sendai, 1982) p. 1365.
22. I. W. DONALD, S. H. WHANG, H. A. DAVIES and B. C. GIESSEN, *ibid* p. 1377.
23. S. S. BRENNER, *J. Appl. Phys.* **27** (1956) 1484.
24. M. NAKA, S. TOMIZAWA, T. WATANABE and T. MASUMOTO, Proceedings of 2nd International Conference on Rapidly Quenched Metals, Cambridge, November 1975 (MIT Press, Cambridge, Mass. 1976) p. 273.
25. H. S. CHEN and J. T. KRAUSE, *Scripta Metall.* **11** (1977) 761.
26. H. S. CHEN, *J. Appl. Phys.* **49** (1978) 3289.
27. H. S. CHEN, A. INOUE, J. T. KRAUSE and T. MASUMOTO, to be submitted.
28. F. E. LUBORSKY, H. H. LIEBERMANN and J. L. WALTER, Proceedings of the Conference on Metallic Glasses, Budapest, 1980.
29. S. KAVESH, "Metallic Glasses" (ASM, Metals Park, Ohio, 1978) p. 36.
30. J. ISHIHARA, private communication, Hitachi Research Laboratory, Hitachi Ltd, Hitachi 317, Japan (1982).
31. T. MASUMOTO, A. INOUE, M. HAGIWARA, I. OHNAKA and T. FUKUSAKO, Proceedings of the 4th International Conference on Rapidly Quenched Metals, Sendai, August 1981, edited by T. Masumoto and K. Suzuki (The Japan Institute of Metals, Sendai, 1982) p. 47.

Received 1 November 1982
and accepted 4 February 1983